

# Device Simulator Calibration for Quartermicron CMOS Devices

T. Grasser, R. Strasser, M. Knaipp, K. Tsuneno<sup>†</sup>, H. Masuda<sup>†</sup>, and S. Selberherr

Institute for Microelectronics, TU Vienna  
Gusshausstr. 27–29, A-1040 Vienna, Austria

<sup>†</sup>Hitachi, Ltd., 16-3, Shinmachi 6-Chome  
Ome-shi, Tokyo 198-8512, Japan

## Abstract

We present the calibration of a device simulator for a 0.25  $\mu\text{m}$  CMOS technology using response surface methodology. For this process several measurements for different gate lengths (0.2–4.0  $\mu\text{m}$ ) were made. Care was taken to eliminate the statistical variations typical to sub-micron devices by measuring several chips on the the same wafer and taking an average sample. The simulations carried out with the calibrated parameters show an error smaller than 2.4% for both the long-channel and the short-channel device.

## 1. Introduction

During the past decade numerous highly effective simulators for the simulation of semiconductor technology (e.g., [1]), as well as semiconductor devices (e.g., [2]) have been developed. These simulators deliver reasonable and accurate predictions of process and device performance. Nevertheless, the models implemented in these simulators employ a vast number of not too well known parameters. Furthermore, due to the complex nature of the underlying physics, it is very difficult to develop models with parameters that are valid for all operating conditions.

## 2. The Minimos Mobility Model

The process was simulated using TSUPREM4, for the device we used MINIMOS. We focused on the calibration of the mobility model, a description of which can be found in [3]:

$$\mu_n^{LIS} = \frac{\mu_n^{ref} + (\mu_n^{LI} - \mu_n^{ref}) \cdot (1 - F(y))}{1 + F(y) \cdot \left(\frac{S_n}{S_n^{ref}}\right)^{\gamma_n}} \quad (1)$$

$$\mu_n^{LISF} = \frac{2 \cdot \mu_n^{LIS}}{1 + \left(1 + \left(\frac{2 \cdot \mu_n^{LIS} \cdot F_n}{v_n^{sat}}\right)^{\beta_n}\right)^{1/\beta_n}} \quad (2)$$

Here,  $\mu_n^{LI}$  considers the ionized impurity scattering,  $\mu_n^{LIS}$  adds the surface scattering, and  $\mu_n^{LISF}$  gives the final mobility including high-field reduction.  $F_n$  represents the driving force for electrons and the pressing force  $S_n$  is equal to the magnitude of the normal field strength at the interface, if the carriers are attracted by the interface, otherwise zero. The depth dependence is modeled as follows:

$$F(y) = \frac{2 \cdot \exp\left(-\left(\frac{y}{y^{ref}}\right)^2\right)}{1 + \exp\left(-2 \cdot \left(\frac{y}{y^{ref}}\right)^2\right)} \quad (3)$$

with  $y$  as distance to the interface. The surface scattering and high-field mobility parameters might depend on the fabrication process (interface quality). To yield physically meaningful results, valid for a large range of gate lengths, appropriate devices and bias conditions must be selected during the calibration. After disabling the high-field mobility degradation term, the error in the maximum drain current of the 4  $\mu\text{m}$  device was found to be about 2%. Hence, it was decided to calibrate the surface mobility parameters using this long-channel device. With these values, the calibration of the high-field mobility parameters was carried out with the short-channel device, where a strong high-field degradation can be expected. It is important to note that non-local effects such as velocity overshoot have been identified as negligible in the particular technology under investigation.

### 3. Calibration

Before performing any calibrations on the 4  $\mu\text{m}$  device, the simulation results obtained by using the default mobility parameters were compared with measurements. To account for the unknown interface charges, the work function difference was adjusted to  $E_w = -0.6$  eV to reproduce a current of  $I_d(V_{th}) = 10$  nA for the measured threshold voltage of  $V_{th} = 0.15$  V (device width is 15  $\mu\text{m}$ ), since the influence of the surface and high field mobility parameters on the drain current are negligible under these bias conditions. As expected, the comparison shows good agreement for the sub-threshold region, whereas the drain current for maximum bias is overestimated by 17%.

#### 3.1. Surface Mobility Parameters

After a sensitivity analysis for the three surface mobility parameters  $\mu_n^{ref}$ ,  $y^{ref}$ , and  $\gamma_n$  for the 4  $\mu\text{m}$  device, the ranges for a central composite circumscribed design [2] were set up. The calibration was automatically run using our VISTA framework [3] with fifteen operating points selected from the measured IV-curves. Using the optimized parameters for the simulation, the resulting maximum absolute error in the drain current was found to be less than 2.3% in the entire range.

#### 3.2. High Field Parameters

For the optimization of the high-field parameters  $S_n^{ref}$ ,  $v_n^{sat}$ , and  $\beta_n$ , the selected fifteen operating points for the 0.25  $\mu\text{m}$  device were restricted to the high bias region. With the optimized values the simulation shows a very small error (0.7%) for the higher bias conditions and a little larger error (2.4%) for intermediary bias conditions. The

Parameter	Optimum	Default	Deviation[%]	Unit
$\mu_n^{ref}$	538	638	-15.7	cm <sup>2</sup> /Vs
$\gamma_n^{ref}$	3.96	10	-60	nm
$\gamma_n$	1.33	1.69	-21.3	1
$S_n^{ref}$	5.933e7	7e7	-15.2	V/m
$v_n^{sat}$	1.48e7	1.45e7	2	cm/s
$\beta_n$	2.217	2	10.8	1

Table 1: Mobility model parameters.

optimum found is summarized in Table 1. All parameters show physically sound deviations from their respective default values. Since there are many uncertainties in the exact doping profile, gate length, etc., the calibrated parameters reflect the average variations of these process parameters.

To test the accuracy of these values for devices with even shorter gate lengths, simulations with the 0.2  $\mu\text{m}$  device were carried out. Again, the accuracy is very good considering the large uncertainty of the process data for such small gate lengths. The final results for the  $L_g = 4 \mu\text{m}$ ,  $L_g = 0.25 \mu\text{m}$ , and the  $L_g = 0.2 \mu\text{m}$  devices using the calibrated values are shown in Fig. 1–Fig. 3.

#### 4. Conclusion

All parameters show physically sound deviations from their respective default values. It is to note, that the large deviation of -60% in the surface parameter  $\gamma_n^{ref}$  denotes the improvement in process technology compared to typical processes investigated in [3]. It is worthwhile to mention, that the saturation-velocity which is a quite firm quantity in terms of physical reasoning, was just marginally adapted by the automatic optimization procedure. Since there are many uncertainties in the exact doping profile, gate length, etc., the calibrated parameters reflect the average variations of these process parameters.

#### References

- [1] Technology Modeling Associates, Inc., Palo Alto, CA, *TMA TSUPREM-4, Two-Dimensional Process Simulation Program, Version 6.2*, June 1995.
- [2] C. Fischer, P. Habaš, O. Heinrichsberger, H. Kosina, P. Lindorfer, P. Pichler, H. Pötzl, C. Sala, A. Schütz, S. Selberherr, M. Stiftinger, and M. Thurner, *MINI-MOS 6 User's Guide*. Institut für Mikroelektronik, Technische Universität Wien, Austria, Mar. 1994.
- [3] S. Selberherr, W. Hänsch, M. Seavey, and J. Slotboom, "The Evolution of the MINIMOS Mobility Model," *Solid-State Electron.*, vol. 33, no. 11, pp. 1425–1436, 1990.

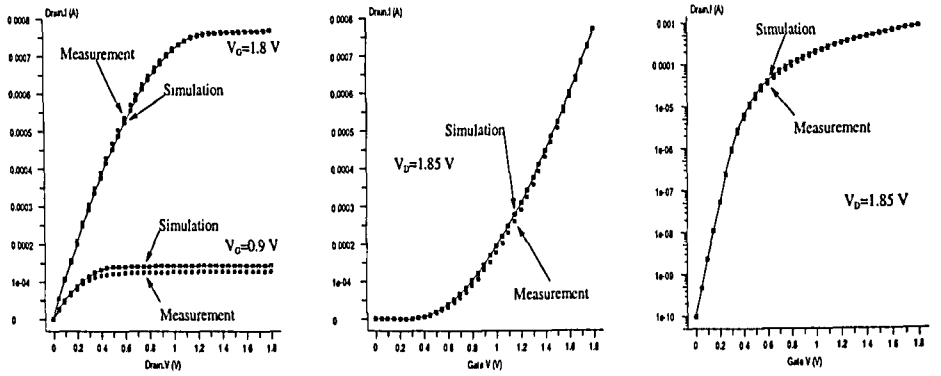


Figure 1: Comparison of simulation and measurement for the  $L_g = 4 \mu\text{m}$  device.

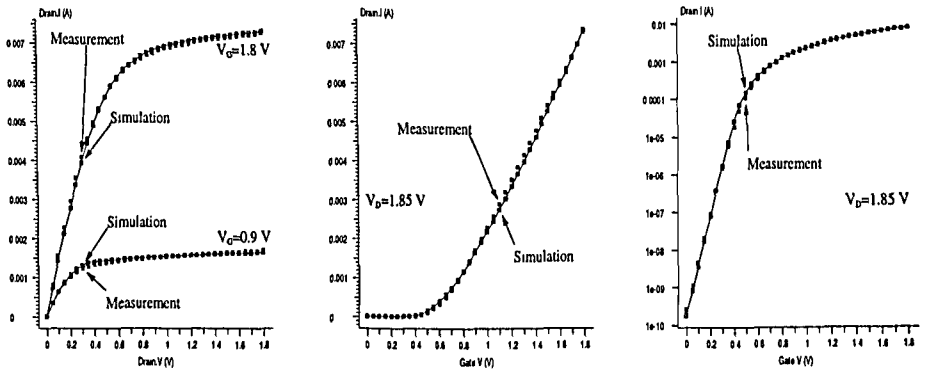


Figure 2: Comparison of simulation and measurement for the  $L_g = 0.25 \mu\text{m}$  device.

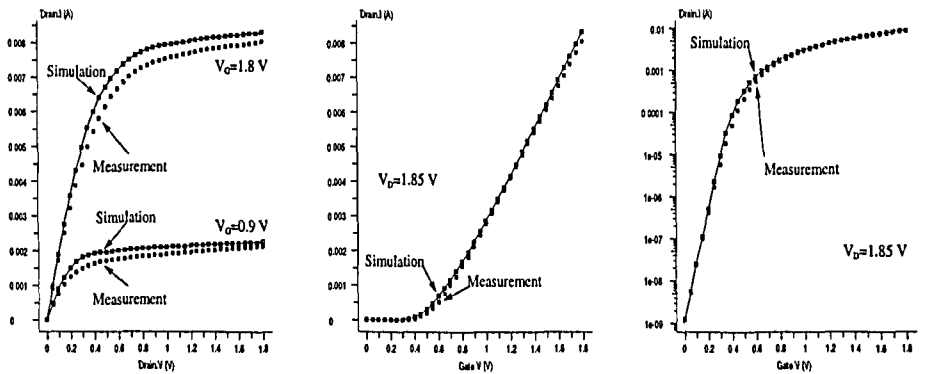


Figure 3: Comparison of simulation and measurement for the  $L_g = 0.2 \mu\text{m}$  device.